Fiber-Bragg-Grating Coupled Magnetostrictive Sensors for Magnetic Tracking of Biomedical Implants

Mahdieh Shojaei Baghini[1], *Graduate Student Member IEEE*, Kristiaan Broekens[2], Michiel Oderwald[2], Paul Breedveld[3], Hadi Heidari[1], *Senior Member IEEE* and Maurits van der Heiden[2]

1. Microelectronics Lab, James Watt School of Engineering, University of Glasgow, Glasgow G12 8QQ, UK
2. Netherlands Organisation for Applied Scientific Research, TNO, Delft, 2628 CK, the Netherlands
3. Delft University of Technology, Delft, 2628 CN, the Netherlands

***Abstract*—Magnetostrictive strain sensors with high spin-orbit coupling have been integrated with Fiber-Bragg-Grating sensors wherein the gap within the gratings varies with strain within the encapsulating magnetostrictive material. Terfenol-D has been chosen as the mm sized magnetostrictive material which exhibits the largest known bulk magnetostriction. The setup utilised consists of an optical to electrical transducer leading to lower noise in the system while carrying out sensing in the magneto-optic domain. Non-linear isotropic analytical modeling and linear anisotropic finite element modeling is carried out to gain further insight into the variation of material parameters with external magnetic field intensity. The operated magnetic fields lie within 100 µT with a sensor sensitivity of 0.6 kHz/ppm, thus reducing risks due to any prolonged or repeated exposure. This technology can be integrated with state-of-the-art sensors with high sensitivity to create smaller and safer tracking systems, particularly in-vivo.**

Keywords—magnetostrictive sensors, implants, Fiber Bragg Grating, magnetic fields, multiphysics, magnetostriction

I. INTRODUCTION

Electromagnetic tracking is currently a key innovation in the area of position detection. Recently paving its way into the biomedical sector, it generates live tracking data based on instrument position and is a prospective alternative to image guided tracking systems which more often than not, require high doses of radiation such as in x-ray fluoroscopy [1, 2] . Sensors placed within the radius of the field generator have the ability to track the position of the needle/medical instrument upon which they are placed. The magnetic flux density changes with the position of the sensor as well as its orientation. This provides a robust and efficient method to track instrument position, primarily during surgery due to a fast response time. This technology can be integrated with state-of-the-art sensors with very high sensitivity in order to create smaller and safer tracking systems, particularly in the in-vivo domain. Magnetic field based tracking systems have gained recent traction for implantable development due to lower cost and better misalignment accuracy wherein a direct line of sight is not necessary for transmission and reception of magnetic fields [3]. In order to provide fine control, it is of paramount importance to track implanted devices with high spatial resolution down to the micrometre range.

This paper is partly supported by UKRI Horizon Europe Guarantee HORIZON-EICPATHFINDERCHALLENGES CROSSBRAIN (GA n.101070908).

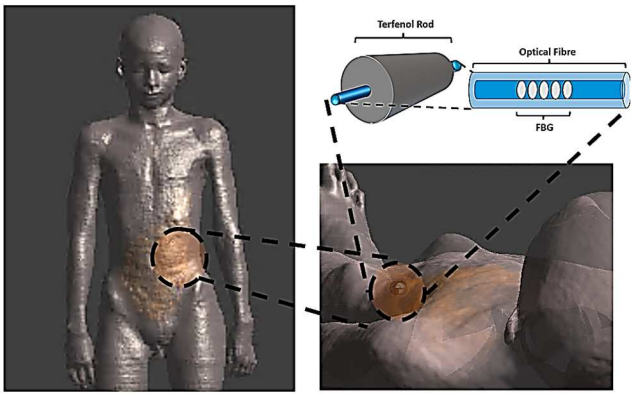

Fig. 1: Schematic of implantable Fiber-Bragg-Grating placed inside a magnetostrictive rod. The spacing between the gratings varies with external magnetic field due to strain developed in the rod.

Magneto-optic composites have been developed, exploiting the high sensitivity of magnetostrictive materials to external magnetic fields of low amplitudes (down to µT) [4]. The strain in the aforementioned devices is then coupled to the reflection spectrum of a Fiber-Bragg-Grating (FBG) sensor which is shifted due to deformation of the optical fiber encapsulated by the magnetostrictive material. Magnetostriction is a property associated with some materials such as Terfenol, Galfenol and Metglas, wherein strain is introduced in the material on exposure to an external magnetic field due to a high degree of spin-orbit coupling [5]. This behaviour is translated to a wavelength shift in an FBG strain sensor epoxy-glued within the magnetostrictive rod (along the axis of maximal strain). Due to the change in the length of the rod, the gratings are displaced leading to a shift in the wavelength of the reflected optical spectrum [6].

The multifaceted modelling of magnetostrictive materials is necessary to predict response prior to experimentation. Analytical as well as numerical models of magnetostriction have been developed via linear and non-linear isotropic and anisotropic formulations [7-9]. In this paper, we explore the role of isotropic analytical modelling and anisotropic finite element modelling in Section II followed by discussion of experimental details in Section III and concluding remarks in Section IV.

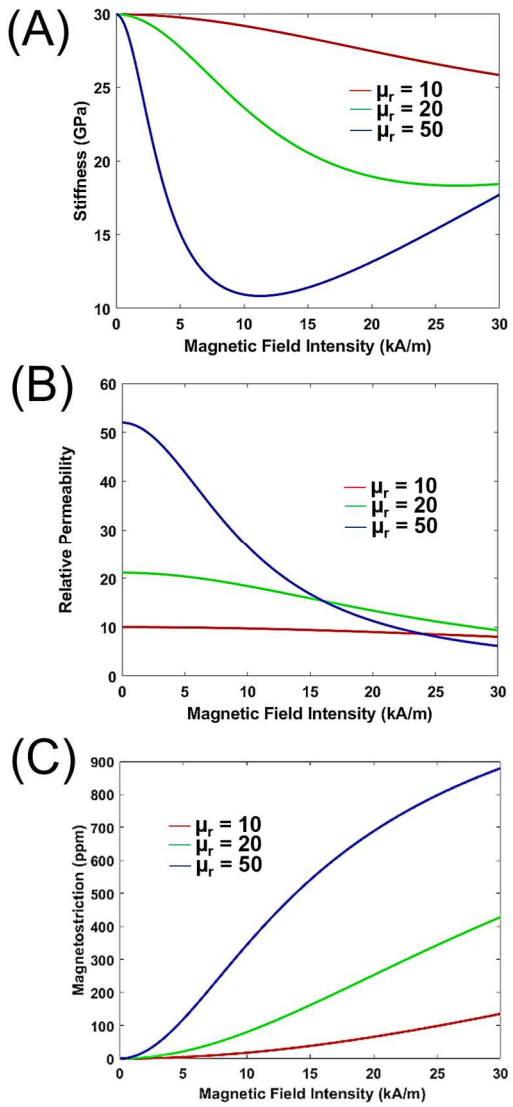

Fig. 2: Variation in A) Stiffness, B) Relative permeability and C) magnetostriction of a Terfenol-D rod with varying external magnetic field intensity and initial magnetic permeability.

II. MODELING AND SIMULATION

A. *Isotropic Analytical Modeling*

Due to the coupling between the mechanical and magnetic responses in magnetostrictive materials, the properties of the Terfenol-D sensor are highly variable with the magnitude of applied magnetic field, pre-stress and temperature. Additionally the permeability and the Young's modulus vary with the external field. It must also be noted that while the pre-stress is considered to be zero, internal stresses are developed within the material which additionally form the basis for the material's continually changing properties and exhibit non-linear characteristics. The basis for modelling is based on Gibbs free energy and is particularly useful under high magnetic fields wherein the spin-orbit coupling is no longer in the linear regime [10]. At no pre-stress, the strain (ε), in the material as a function of magnetisation (M) is given by (1).

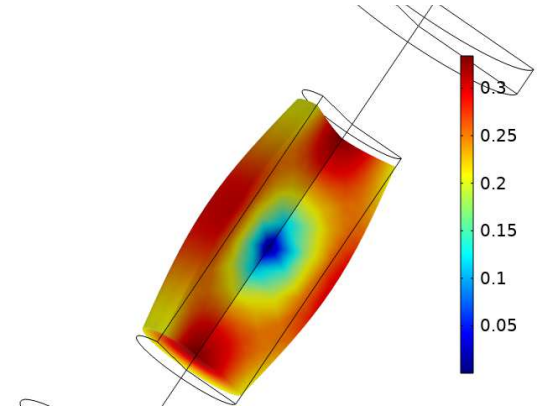

Fig. 3: Compressive displacement in magnetostrictive rod (in μm) when 1A is applied to the DC coil and the AC coil is held at a peak voltage difference of 1V

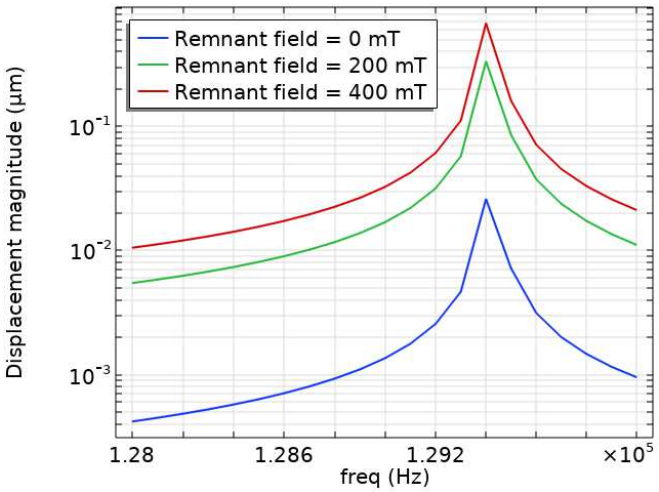

Fig. 4: Frequency dependent magnetostriction in the Terfenol-D rod as a function of peak current through DC coil .

$$\epsilon = \lambda_s \frac{M^2}{M_s^2} \quad (1)$$

Wherein M_s is the saturation magnetisation of the materials and λ_s is the strain developed in the material at saturation. Due to the rotation of magnetic boundaries as well as internal stresses developed in the material, the Young's modulus as well as the relative permeability change with the magnetic field intensity. At no magnetic excitation, the calculated Young's modulus is 29.9 GPa and the supplier provided isotropic Young's modulus is 30 GPa, further confirming the validity of the constitutive relations developed in [10] for our materials. The trend of the stiffness, relative permeability and magnetostriction of a bulk magnetostrictive rod is shown in Fig. 2 at different susceptibilities of the material. It must be noted that while the maximum permeability of the utilized rods is 10, analytical simulations at higher permeabilities have been carried out to further highlight the non-linearities in material properties. It can be seen that the peak achievable magnetostriction for a Terfenol-D rod is 100 ppm at a given constant DC magnetic bias for a relative permeability of 10. To extract the complete spectrum

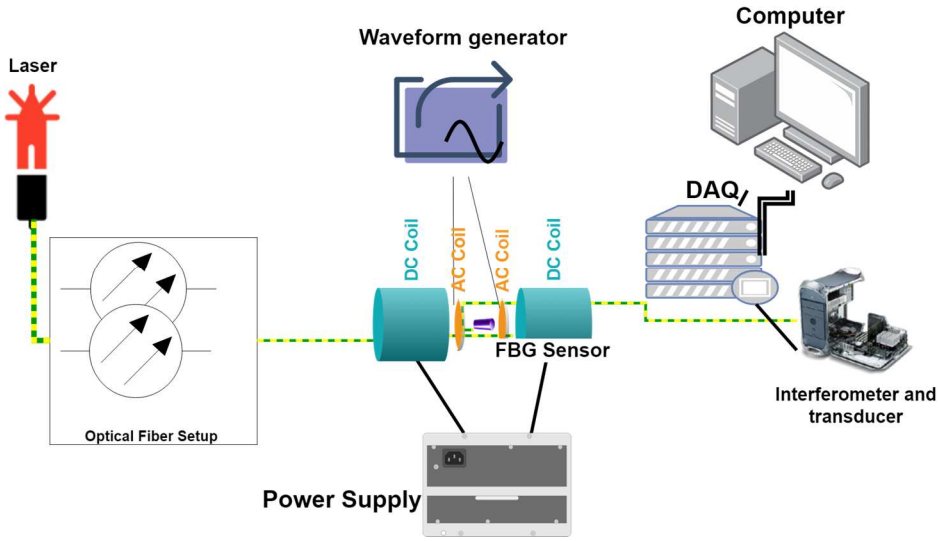

Fig. 5: Experimental setup constituting of FBG-Terfenol sensor

of properties of the magnetostrictive tensor this DC bias is chosen for frequency domain numerical analysis as explained in sub-section II.B. While the analytical studies provide insight into variation of magneto-mechanical properties, they do not account for magnetic anisotropy in the crystal make-up. Furthermore, it is perturbation of the magnetic field around the bias that leads to a change in magnetostriction and is further taken account during numerical modeling.

B. Anisotropic numerical modeling

Terfenol-D is intrinsically not isotropic and for more accurate results, its anisotropic nature must be taken into account. This has been done in COMSOL using an extended form of Hooke's law. The linear anisotropic constitutive relationships of the solid mechanics and magnetic fields physics are fully coupled together and the initial condition of zero pre-stress has been chosen.

2D axisymmetry has been chosen to reduce computation time and complexity. The study under consideration is a frequency domain study with the frequency ranging from 10 kHz to 200 kHZ in steps of 50 kHz. The Terfenol-D rod has a diameter of 2 mm and a length of 10 mm, as in the experiments. The compressive strain in the rod is shown in Fig. 3 when super-imposing magnetic fields are applied in the direction of the easy-axis of the rod. The magnetostriction as a function of frequency (in the vicinity of the resonance frequency) is shown in Fig. 4 and the increase in magnetostriction can be clearly observed with rising DC amplitude. The aforementioned effects are more pronounced at resonance (~ 129 kHz). The peak value of strain at similar biasing conditions as the analytical model leads to a magnetostriction of ~60 ppm leading to similar orders of magnitude as the analytical model and numerical model. A secondary but significant advantage to numerical modeling is the consideration of the skin-depth effect with rising frequency which plays a paramount role in deciding the thickness of the sensor.

III. EXPERIMENTAL STUDIES

The experimental setup is shown in Fig. 5 constituting of an optical fiber setup consisting of a 1550 nm laser as the primary light source of which the operating power is set to 60 mW. Three optic couplers are placed at each receiving and transmitting sections of the setup which almost equally split the energies between two fibers. Thereon after, the light is reflected by an optical sensor placed within the Terfenol-D rod. To further remove higher order harmonics, the light is passed through an optical filter which is an FBG with a wide peak. At the final stage another configuration of the Y-coupler is utilised to combine the energies. The principle of operation, as explained previously, is the dependency of the Bragg peak position which depends on the strain of the magnetostrictive rod. To make detection more efficient, the

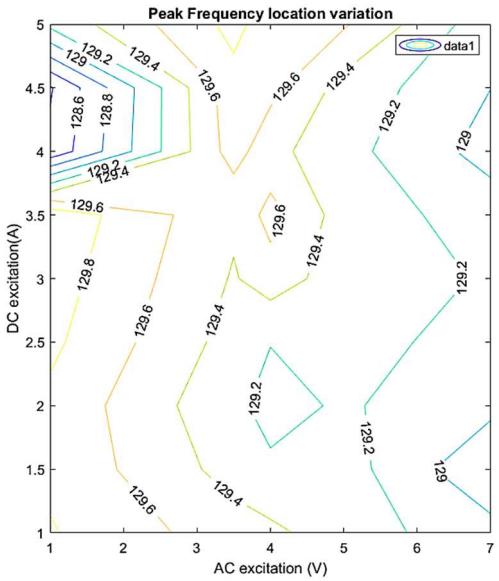

Fig. 6: Contour map of experimental variation of resonance frequency with DC and AC bias.

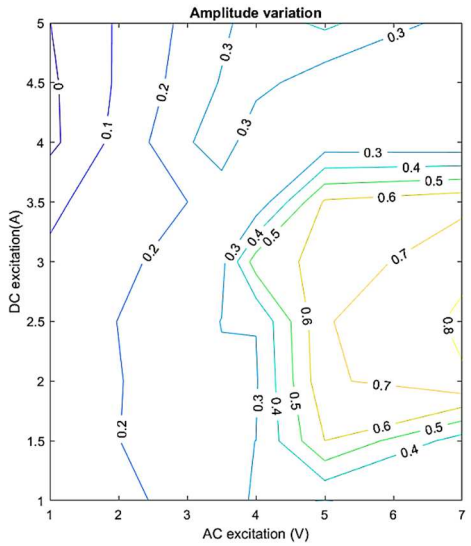

Fig. 7: Contour map of experimental variation of electrical signal with direct dependence on interferometry output.

signal is first passed through a three-phase interferometer after which it is transduced to an electrical signal. The sensor FBG constitutes of 80 µm clad fiber with a FWHM of 0.11 +/- 0.01 nm and the optical fiber constitutes of 125 µm clad fiber with a FWHM of 2 +/- 0.01 nm.

The Terfenol-D rod is mounted in the centre of a concentric Helmholtz coil arrangement consisting of DC and AC coils driven by a power supply and a function generator, respectively. The AC field has been generated via a sinusoidal linear chirp signal in MATLAB. The duration and frequency range of the sweep have been generated in such a way that the maximum amount of energy imparted to the sensor falls within its resonance frequency range. The data acquisition system was utilised to record the optical signal from the optical fiber which is spliced with the fiber housed within the sensor. The electrical signal from the reference coil and the arbitrary waveform generator have been acquired as well. The AC field is superimposed on this DC field so as to shift the point of operation to the linear region of magnetostrictive operation. The transduced signals are recorded by the data acquisition system and post-processing is carried out in MATLAB involving the Fourier transform of the recorded signal followed by Gaussian curve fitting. After carrying out measurements at the range specified in Fig. 4a sensitivity of 0.6 kHz/ppm is observed in the resonance peak shift in the presence of a constant external field of ~100 µT. The experimental values of strain lie within 0-10 ppm while that of the analytical and numerical values lie within 50-100 ppm under the fields of interest. This lowered strain is observed due to the confounding effects of damping in the material due to the presence of bonding epoxy as well as the finite skin-depth at higher frequencies reducing the peak value of magnetic field at the centre of the rod where the FBG is placed. Improved models are being developed to take into account the lowered strain transfer to the magnetostrictive material under different binding agents and encapsulants. It can be seen that the average resonance of frequency computer numerically is in good agreement with the experimental frequencies shown in Fig. 6. In order to predict the variation of frequency a fully coupled numerical model is being developed as opposed to the current unidirectional model.

IV. Conclusion

In this paper, a magneto-optical device based on magnetostrictive-FBG composite strain sensors is introduced. Isotropic and anisotropic modeling of magnetostriction have been explored as suitable design frameworks as well as initial experimentation of mm-sized implants consisting of bulk Terfenol-D rods. The sensitivity of the sensors in terms of resonance frequency shift has been derived experimentally as 0.6 kHz/ppm in AC magnetic fields less than 100 µT which fall within biomedical regulations and reduces risks due to prolonged exposure.

References

[1] A. Sorriento *et al.*, "Optical and Electromagnetic Tracking Systems for Biomedical Applications: A Critical Review on Potentialities and Limitations," *IEEE Reviews in Biomedical Engineering,* vol. 13, pp. 212-232, 2020, doi: 10.1109/RBME.2019.2939091.

[2] N. E. Shalom, G. X. Gong, and M. Auster, "Fluoroscopy: An essential diagnostic modality in the age of high-resolution cross-sectional imaging," (in eng), *World J Radiol,* vol. 12, no. 10, pp. 213-230, Oct 28 2020, doi: 10.4329/wjr.v12.i10.213.

[3] S. Tarantino, F. Clemente, D. Barone, M. Controzzi, and C. Cipriani, "The myokinetic control interface: tracking implanted magnets as a means for prosthetic control," *Scientific Reports,* vol. 7, no. 1, p. 17149, 2017/12/07 2017, doi: 10.1038/s41598-017-17464-1.

[4] Y. Suwa, S. Agatsuma, S. Hashi, and K. Ishiyama, "Study of Strain Sensor Using FeSiB Magnetostrictive Thin Film," *IEEE Transactions on Magnetics,* vol. 46, no. 2, pp. 666-669, 2010, doi: 10.1109/TMAG.2009.2033553.

[5] B. Yoo, S.-M. Na, A. B. Flatau, and D. J. Pines, "Directional magnetostrictive patch transducer based on Galfenol's anisotropic magnetostriction feature," *Smart Materials and Structures,* vol. 23, no. 9, p. 095035, 2014/08/14 2014, doi: 10.1088/0964-1726/23/9/095035.

[6] F. Casagrande, P. Crespi, A. M. Grassi, A. Lulli, R. P. Kenny, and M. P. Whelan, "From the reflected spectrum to the properties of a fiber Bragg grating: a genetic algorithm approach with application to distributed strain sensing," *Appl. Opt.,* vol. 41, no. 25, pp. 5238-5244, 2002/09/01 2002, doi: 10.1364/AO.41.005238.

[7] B. Dai, Z. He, Z. Yang, J. Zhou, G. Xue, and G. Liu, "Modeling and analysis of the piezomagnetic, electromagnetic, and magnetostrictive effects in a magnetostrictive transducer," *AIP Advances,* vol. 11, no. 12, p. 125213, 2021/12/01 2021, doi: 10.1063/5.0057715.

[8] P. A. Sánchez, O. V. Stolbov, S. S. Kantorovich, and Y. L. Raikher, "Modeling the magnetostriction effect in elastomers with magnetically soft and hard particles," *Soft Matter,* 10.1039/C9SM00827F vol. 15, no. 36, pp. 7145-7158, 2019, doi: 10.1039/C9SM00827F.

[9] Y. Li, J. Zhu, Y. Li, H. Wang, and L. Zhu, "Modeling dynamic magnetostriction of amorphous core materials based on Jiles–Atherton theory for finite element simulations," *Journal of Magnetism and Magnetic Materials,* vol. 529, p. 167854, 2021/07/01/ 2021, doi: https://doi.org/10.1016/j.jmmm.2021.167854.

[10] D.-G. Zhang, M.-H. Li, and H.-M. Zhou, "A general one-dimension nonlinear magneto-elastic coupled constitutive model for magnetostrictive materials," *AIP Advances,* vol. 5, no. 10, p. 107201, 2015/10/01 2015, doi: 10.1063/1.4933024.